

Hotter Electrons and Ions from Nano-structured Surfaces

S. Bagchi*, P. Prem Kiran, M.K. Bhuyan, S. Bose, P. Ayyub, M. Krishnamurthy and
G. Ravindra Kumar

Tata Institute of Fundamental Research, 1 Homi Bhabha Road, Colaba, Mumbai-400005,
India
email: suman@tifr.res.in

Abstract

The impact of nano-structured surfaces on particle generation from ultrashort intense laser produced plasmas is presented over an intensity range of $10^{15} - 10^{17} \text{ Wcm}^{-2}$. The nano-structured surface evidently produces hotter plasma but *does not* lead to the generation of hotter ions, a counterintuitive result based on present understanding of plasma expansion mechanism. Although the total ion flux and energy is more in the case of structured surfaces, the average energy of the projectiles is found to be lower than that from polished surfaces. The nano-structured surface shows preferential enhancement of lower energy ions and an intensity dependent divergence of the ejected particles.

1. Introduction

Recent advances in the field of ultrashort intense (USI) solid state lasers has enabled us to investigate matter under extreme conditions [1]. Under the influence of the strong laser pulse the matter instantly ionizes to form overdense plasma, a rich source of photons of different wavelengths and particles with a wide range of energy and charge [2]. Generation of huge accelerating field, current densities and particle flux over an ultrashort duration makes laser plasma based particle sources very interesting from fundamental aspects as well as for potential applications [3 - 5]. When an USI laser pulse is focused on the target, rapid ionization takes place in the initial part of the pulse and the electrons generated in this process interacts with the laser photons to couple more laser energy in to the system via collisional as well collisionless processes like resonance absorption (RA), vacuum heating (VH) etc.[6, 7]. This gives rise to a bunch of highly energetic electrons distinctly separated from the large pool of relatively colder electrons present in the plasma. These high energetic electrons come out of the quasineutral plasma inducing a positive charge resulting in generating a strong electric field responsible for acceleration of ions to very high energy within a very short duration. This acceleration mechanism has been vigorously tested in experiments as well as in numerical simulations [8 - 11]. In this perspective efficient coupling of laser energy into the plasma is crucial. Recent experiments involving nano-structured surfaces, microdroplets, clusters have reported enhanced laser energy coupling up to 80 % by judicious choice of targets parameters [12 - 14]. The aim of this study is to find out whether similar target optimization scheme also works for the generation of high energy ions or not. To this extent, we report the influence of surface modulations created by nano-particles coated on a polished metal surface on the characteristics of ion emission in the keV to MeV range.

2. Experimental details

The schematic experimental arrangement is shown in Fig. 1(a). The target is irradiated by 50 fs, p-polarized laser pulse from a 806 nm, Ti-Sapphire laser (THALES LASER, ALPHA 10) with a contrast ratio of 10^6 : 1 for fs to the ns pedestal, focused by an off axis parabolic mirror in f/4 focusing geometry to a focal spot size of $10 \mu\text{m}$ as determined from equivalent imaging technique giving a peak intensity of $10^{15} - 8.0 \times 10^{16} \text{ Wcm}^{-2}$. The pulse-to-pulse intensity fluctuation is kept within 5%. A motorized x-y- θ -z stage assembly (z being

the laser propagation direction and θ being the rotation angle with respect to vertical (y-) axis) ensures that the laser pulse always hits a fresh target region. The target used in this experiment is a polished copper (Cu) block ($50 \times 50 \times 5$ mm), half of which is coated with $0.2 \mu\text{m}$ layer of ellipsoidal Cu nanoparticles (CuNP). The nano-particles are deposited using high pressure DC- magnetron sputtering technique [15]. The average size of the nano-particles as determined from the Scherrer broadening technique of the Cu (111) x-ray diffraction line is 15 nm with an aspect ratio of 1.5. The half coated target ensures identical experimental conditions for polished Cu and CuNP coated surface. With all the components inside the base pressure of the experimental chamber is $\sim 10^{-6}$ torr.

The bremsstrahlung spectra in the 20 - 200 keV energy range is collected by a properly calibrated NaI(Tl) detector, covered with 15 mm thick layer of lead and gated in time with the incident laser pulse to ensure a nearly background free data acquisition. The signal from the detector is first amplified then recorded with a multichannel analyzer connected to computer by RS-232 interfacing protocol. The transmission factor of viewport of the experimental chamber has been taken into account while analyzing the data. In order to reduce piled up events the count rate was kept below 0.1 per laser shot by properly positioning the detector and keeping suitable lead apertures in front of it. The ion energy is measured with conventional time of flight (TOF) measurement technique with a channel electron multiplier (CEM) placed at a distance of 97 cm from the plasma spot subtending a solid angle of 26 msr. The TOF assembly is kept at a steady pressure of $\sim 10^{-7}$ torr by differential pumping to avoid any damage to CEM due to unwanted avalanche processes. The arrival time information is stored in the computer via 1GHz digital oscilloscope (YOKOGAWA DL7200) interfaced to the computer following GPIB interfacing protocol. To measure the total ion flux a large area (230 cm^2) Faraday cup (LAFC) biased at a voltage of -300 V is placed at a distance of 35 cm from the plasma spot. The LAFC consists of $10 \mu\text{m}$ thick Aluminium foil to preferentially stop heavy ions [16]. A nickel mesh biased at a biasing voltage of -500 V is placed right in front of the LAFC to suppress the secondary electron emission from the foil. To estimate the angular divergence of the emitted ions from the plasma, LAFC is replaced with four annular Faraday cups (AnFCs) placed at angles of 4.6, 8.1, 11.6 and 16.6 degrees from the axis of the TOF (Fig. 1(b)). Each AnFC is made of 2 mm thick copper sheets and is biased at a voltage of -300 V.

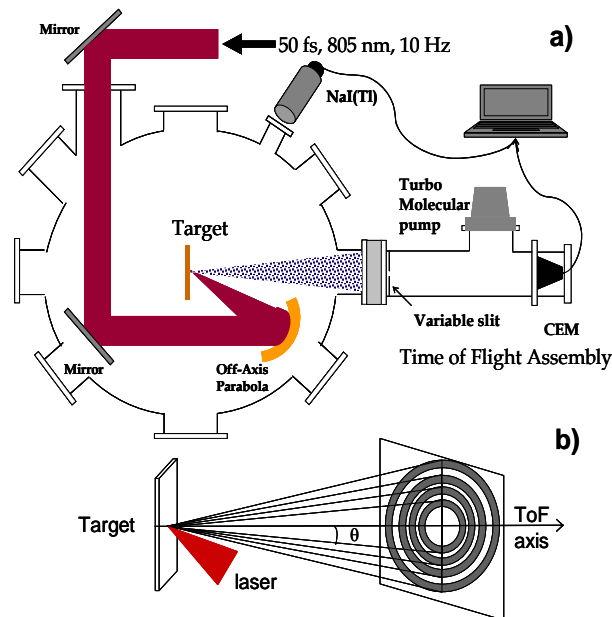


Fig. 1 Schematic diagram of the (a) experimental set up; (b) annular FCs (AnFC).

3. Results

The bremsstrahlung spectra for polished Cu and CuNP are shown in the inset of Fig. 2. The hot electron distribution for polished Cu is found out to be 9.3 ± 1.1 keV, whereas for CuNP a bi-Maxwellian electron distribution is obtained with temperatures of 9.5 ± 1.7 keV and 33.9 ± 6.4 keV clearly showing increased laser energy coupling into the plasma, in tune with the previous observations [12]. The integrated x-ray energy yield emitted in the range of 20 – 200 keV is found out to be 2.9×10^{-9} and 7.5×10^{-9} mJ for polished Cu and CuNP coated surface respectively. The ratio of the hard x-ray yield from CuNP coated surface to polished Cu surface (Fig. 2) over the entire laser energy range used in this experiment is always greater than unity reinforcing the enhanced energy coupling to the plasma. As the intensity is increased the ratio is found to decrease. This is due to the possible “blasting off” of the CuNP layer from the copper surface [17].

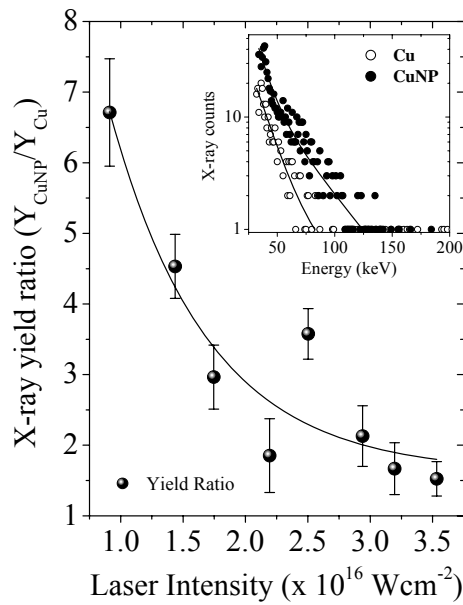


Fig. 2 Ratio of the hard x-ray yield from CuNP coated surface and polished Cu surface. The inset shows bremsstrahlung spectra for CuNP (solid circles) and polished Cu (open circles) surface.

A typical ion energy spectrum obtained at laser energy of 2.3 mJ is shown in Fig.3 (a), where $n(E)$ implies number of particles having energy lying between E to $E + dE$. Evidently the TOF spectrum of CuNP is characteristically different from polished Cu. The Cu TOF spectrum shows a single Maxwellian distribution, whereas, the CuNP spectrum shows a bi-Maxwellian distribution (inset of Fig. 3(a)), similar to the electron energy distributions obtained from hard x-ray spectra. A clear preferential enhancement of the low energy ions (<75 keV) is observed over the entire range of laser intensities used in the experiment. The ion energy spectra of polished Cu shows a double hump structure at lower laser energy (< 1 mJ) above which the distribution is always single Maxwellian. On the other hand, the ion energy distribution obtained from CuNP shows a triple hump structure which reduces to a double hump structure with the increase in laser. The total ion flux in the low energy range (4 – 75 keV) is considerably higher for CuNP compared to polished Cu surface but in the higher energy side (75 – 1400 keV) the flux is almost half. This behavior is observed for all incident laser energies. Over the entire energy range (4 – 1400 keV) the total ion flux from CuNP is 40 % higher than polished Cu. Similarly, as seen in Fig.3 (b), the total ion energy ($\int En(E) dE$)

in the low energy range is 70 % higher for CuNP (filled squares) whereas it is 60 % lower in higher energy side (filled circles). Over the total energy range the total ion yield seems to be 25 % higher for CuNP (filled triangles).

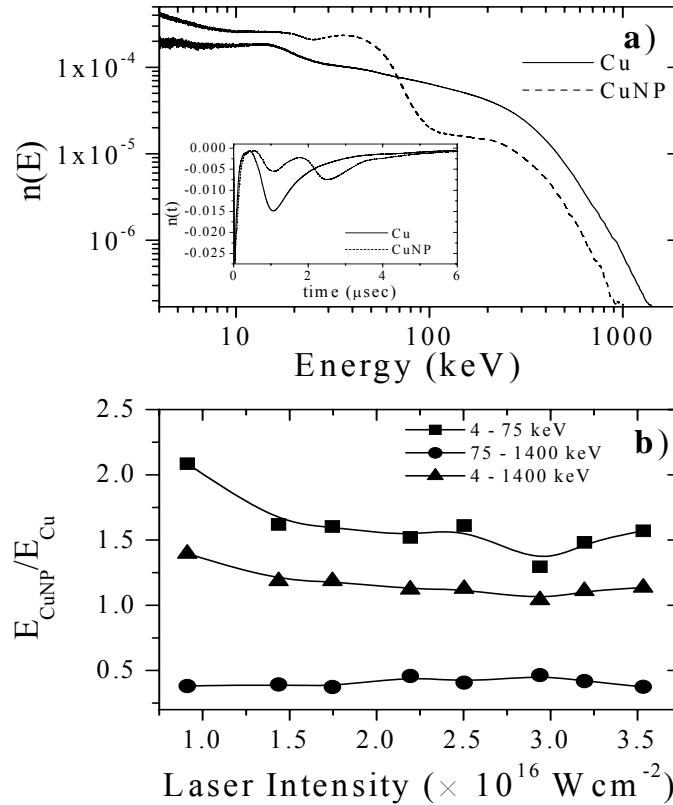


Fig. 3 (a) Typical ion energy spectra from polished Cu (solid line) and CuNP (dashed lines) sample. The inset shows the observed TOF spectra. (b) Ratio of total ion energy emitted from CuNP and polished Cu targets as measured from CEM.

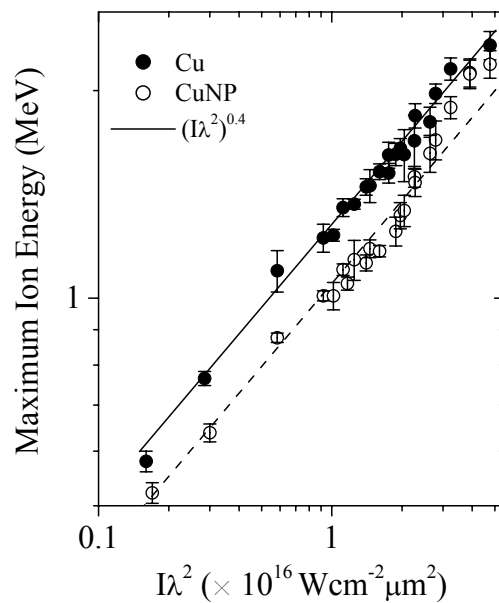


Fig.4: Maximum ion energies obtained from CuNP coated surface and polished Cu surface at different laser intensities. The lines show the scaling of $E_{\text{max}} (\sim (I_l^2)^{0.4})$ for both targets.

Fig.4 depicts the variation of maximum ion energies (E_{\max}) obtained from CuNP and polished Cu surface. Evidently, the maximum energy for CuNP is always lower than polished Cu though E_{\max} scales as $(I\lambda^2)^{0.4}$ following earlier experimental and theoretical simulations [10,11]. The E_{\max} from CuNP varies from 0.5 to 1.6 MeV compared to 0.6 to 2.4 MeV for polished Cu sample indicating a reduction close to 50 %. At higher intensities ($> 3 \times 10^{16} \text{ Wcm}^{-2}$) E_{\max} is almost the same from both the targets possibly due to the blasting off of the CuNPs [17]. The possibility that protons are preferentially absorbing most of the energy is also explored but thorough checking of the TOF spectra rules it out.

To get an estimate of the total ion flux emitted from the laser produced plasma in both cases a LAFC is placed with a nickel mesh in front of it. The total ion flux ratio measured with this shows a reverse trend with CEM as seen in Fig.5(a). As the laser energy increases, the flux ratio as measured by CEM ($\Omega \sim 26 \text{ msr}$) goes down whereas the flux ratio measured by LAFC ($\Omega \sim 2.36 \text{ sr}$) goes up consistently. This may be due to more divergent ion beam from the CuNP target. To confirm the beam divergence we have replaced the LAFC with AnFCs to measure the angular divergence of the emitted ion beam. Fig. 5(b) shows the ratio of the total ion flux measured at different angles by FCs. The figure clearly shows the increased divergence of the emitted ion beams for CuNP. Also with the increase of the laser energy the divergence seems to decrease and becomes similar to that of polished Cu, although the total flux still remain higher. As the laser energy is increased further, the ratio comes closer to unity, a feature that has been seen also in hard x-ray yield (Fig.2) and in E_{\max} (Fig. 4).

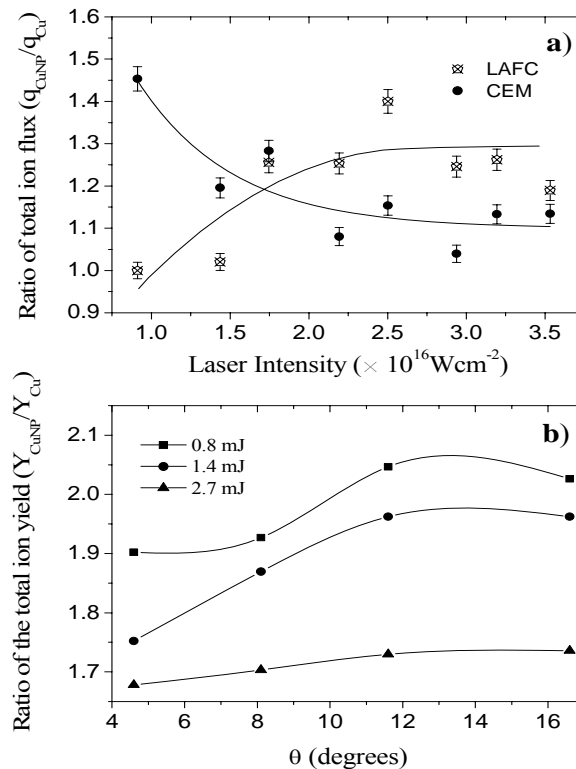


Fig.5 Ratio of the total ion flux from CuNP coated and polished Cu surfaces by (a) LAFC and CEM (b) angular divergence measurement using annular FCs

4. Discussion

The emission of lower energy ions from the nanoplasma indicates that optimizing of the surface to produce hotter electrons “*need not necessarily*” lead to faster ions. The observed effect can be explained qualitatively by the dynamics of the plasma evolution leading to electron and ion generation. The interaction of intense laser with matter produces a large number of electrons out of which a small fraction are energetic enough to escape target even before it is fully ionized. The rest are contained within the target and ionizes the surrounding target medium by collisions and ultimately fill the target volume forming electron sheath responsible for ion acceleration. The magnitude of this field can be expressed as $E_{\text{accl}} = k_B T_e / e \lambda_D \sim (n_h T_h)^{1/2}$ where λ_D is the local Debye length, n_h and T_h being the local density and temperature of the hot electrons. This electric field amplitude can be of the order of 10^{12} V/m strong enough to accelerate ions up to MeV/q energies [8, 18]. In general the plasma expansion from polished surface can be approximated as a one dimensional but this is not the case with NP coated targets as the NPs are distributed over the surface in a random way and hence the plasma expansion is not uniform throughout. The local plasma expansion critically depends on the relative orientation of the number of NPs with respect to the local surface normal, located within the focal spot radius and hence giving rise to a nonplanar plasma expansion. Following the particle-in-cell (PIC) simulations [8], the ion emission from laser produced plasma in solids is mostly directed toward the local target normal, implying the random geometrical orientation of the NPs may be responsible for the enhanced beam divergence as compared to the polished surface.

Experimental studies have revealed that in the low intensity regime the photoelectric emission rate can be greatly enhanced by the excitation of collective modes of the metals, the surface plasmons [19]. Qualitatively the energy of the short laser pulses is stored by the surface plasmon, creating a hot electron population that can not transfer their energy to the lattice [20]. This collective behavior along with their shape dependent “lightning rod” factor [12] effectively reduces the plasma formation threshold laser intensity compared to polished surface. Effectively the intense portion of the laser pulse interacts with preformed underdense plasma and hence being absorbed more efficiently compared to a polished surface. This underdense plasma increases the local scale length of plasma expansion reducing the accelerating sheath potential giving rise to the slower ions from CuNP compared to the polished Cu surface. The reduction in the maximum energy of the protons and ions due to the increased scale length leading to more divergent beam has also been observed [21 – 23].

5. Summary

In summary, we have studied the role of nano-structured surfaces in ion acceleration process from fs laser produced plasma. The study reveals that though the nano-structuring of the surface helps to couple considerably more laser energy to the plasma but does not help in generating high energy ions by effectively reducing the accelerating potential of the sheath layer. The energy dependent divergence of the emitted ion beam measured points towards increased ion beam divergence from nano-structured surfaces. It is therefore necessary to understand the dynamics of the plasma expansion in detail to optimize the particle generation from laser produced plasma sources. Presently more experiments are being carried out with varying shapes and sizes of the nano-structures and under different laser conditions to understand the role of nano-structured surfaces in ion acceleration from laser produced plasma in a better way.

References

1. D. Umstadter, *Phys. Plasmas* 8 (2001) 1774.
2. B. M. Hegelich, B. J. Albright, J. Cobble, K. Flippo, S. Letzring, M. Paffett, H. Ruhl, J. Schreiber, R. K. Schulze, and J. C. Fernandez, *Nature* 439 (2006) 441.
3. V. Malka, *Laser and Particle Beams*, 20 (2002) 217.
4. J. Badziak, A. A. Kozlov, J. Makowski, P. Parys, L. RYC, J. Wolowski, E. Woryna, A.B. Vankov, *Laser and Particle Beams*, 17 (1999) 323.
5. Y. Glinec, J. Faure, J. Fuchs, H. Szymanowski, U. Oelfke, V. Malka, *Med. Phys.* 33 (2006) 155
6. W. L. Kruer, *The Physics of Laser Plasma Interactions*. (New York, Addison-Wesley 1988).
7. F. Brunel, *Phys. Rev. Lett.* **59** (1987) 52.
8. S. C. Wilks, A. B. Langdon, T. E. Cowan, M. Roth, M. Singh, S. Hatchett, M. H. Key, D. Pennington, A. MacKinnon, and R. A. Snavely, *Phys. Plasmas* 8 (2001) 542.
9. P. Mora, *Phys. Rev. Lett.* **90** (2003) 185002.
10. E. L. Clark, K. Krushelnick, M. Zepf, F. N. Beg, M. Tatarakis, A. Machacek, M.I.K. Santala, I. Watts, P. A. Norreys, A. E. Dangor, *Phys. Rev. Lett.* **85** (2000) 1654.
11. A. Zhidkov, A. Sasaki, T. Tajima *Phys. Rev. E* 61 (2000) R2224.
12. P. P. Rajeev, P. Taneja, P. Ayyub, A. S. Sandhu, G. R. Kumar, *Phys. Rev. Lett.* 90, (2003) 115002.
13. S. Ter-Avetisyan, M. Schnurer, S. Busch, E. Risse, P. V. Nickles, and W. Sandner, *Phys. Rev. Lett.* 93 (2004) 155006.
14. T. Ditmire, J. W. G. Tisch, E. Springate, M. B. Mason, R. A. Smith, J. Marangoos, M. H. R. Hutchinson, *Nature* 386 (1997) 54.
15. P. Ayyub, R. Chandra, P. Taneja, A. K. Sharma, and R. Pinto, *Appl. Phys. A* 73 (2001) 67.
16. J. F. Ziegler, SRIM-2003, *Nuclear Instruments and Methods in Physics Research B* 219-220 (2004) 1027; CASINO 2.0 <http://www.gel.usherbrooke.ca/casino/index.html>
17. P. P. Rajeev, S. Kahaly, S. Bagchi, S. Bose, P. P. Kiran, P. Taneja, P. Ayyub, G. R. Kumar, *J. Phys. IV France* 133 (2006) 533.
18. F. Amiranoff, R. Fedosejevs, R.F. Schmalz, R. Sigel and Y. Tung, *Phys. Rev. A* 32 (1985) 3535.
19. V.M. Shalaev, C. Douketus, T. Haslett, T. Stuckless, M. Moskovits *Phys. Rev. B* 53 (1996) 11193.
20. J. Kupersztych, P. Monchicourt, M. Raynaud, *Phys. Rev. Lett.* 86 (2001) 5180.
21. M. Roth, A. Blazevic, M. Geissel, T. Schlegel, T. E. Cowan, M. Allen, J.-C. Gauthier, P. Audebert, J. Fuchs, J. Meyer-ter-Vehn, M. Hegelich, S. Karsch, A. Pukhov, *Phys. Rev. ST* 5, (2002) 061301.
22. A.J. Mackinnon, M. Borghesi, S. Hatchett, M.H. Key, P.K. Patel, H. Campbell, A. Schiavi, R. Snavley, S.C. Wilks, O. Willi, *Phys. Rev. Lett.*, 86 (2001) 1769.
23. A. Maksimchuk, S. Gu, K. Flippo, D. Umstadter, V.Yu. Bychenkov, *Phys. Rev. Lett.*, 84 (2000) 4108.